EXCELLENT PUBLISHERS

International Journal of Current Research and Academic Review

ISSN: 2347-3215 Volume 3 Number 4 (April-2015) pp. 202-210

www.ijcrar.com

Effects of adenine thickness and thermal evaporation rate in organic light-emitting diodes

Seul Gi Kang[1], Han Seong Lee[2], Sang Mok Jung[1], Han Joo Lee[1], Ji Su Son[1], Jae Hyuk Jeon[1] and Hyun Woung Shin[1*]

[1]Department of Life Science and Biotechnology, Soonchunhyang University, Shinchang-myeon, Asan-si, Chungcheongnam-do, 366-745 South Korea
[2]Department of Forensic Investigation, Research Center of National Coast Guard, Korea
Corresponding author

KEYWORDS

Adenine, Biomolecule, Luminance, Vacuum evaporation

A B S T R A C T

An organic light-emitting diode (OLED) device was fabricated with adenine as the electron blocking layer (EBL). The device consisted of a multilayered structure of indium tin oxide/adenine/N,N′-bis(naphthalen-1-yl)-N,N′-bis(phenyl)benzidine/tri(8-hydroxyquinoline) aluminum(III) (ITO/adenine/ NPB/Alq3/Al). The thickness of the ITO, NPB, Alq3, and Al layers remained fixed. The thickness of the adenine layer varied as follows: 1, 2, 4, and 5 nm. Experiments were conducted at adenine deposition rates of 0.5 and 1.1, 0.5 Å $s^{-1}$was shown better performance. Current–voltage and luminance–voltage characteristics were used to determine the efficiency of the device. The highest luminance (24.053 cd m^{-2} at a voltage of 15 V) corresponded to an adenine layer thickness and deposition rate of 4 nm and 1.0 Å s^{-1}, respectively. The results presented are expected to contribute to the development of novel organic light-emitting materials.

Introduction

Significant advances in display device technology have occurred over the years, as evidenced by the cathode ray tube (CRT) that emits electrons to a screen, the liquid crystal display (LCD) that applies an electric signal to a liquid crystal material, electrically charged ionized gases or plasma display panels(PDPs), and more recently organic light-emitting diodes (OLEDs) (Lieberman, 2004).

The brightness of CRTs is excellent; however, these devices are heavy and suffer from high power consumption, large thermal loads, and low luminance (Chen *et al.*, 2009). CRTs are also limited by their phosphor persistence and volume control. LCDs, developed to solve the problems associated with CRTs, require more complex fabrication processes than CRTs but have a slow response rate and a narrow viewing angle (Barbosa and Campos, 2004).

New technology has facilitated the era of high-definition television with the availability of PDPs. PDPs are lightweight for wall-mounting; however, these devices also have a relatively narrow viewing angle and suffer from screen burn-in and high power consumption (Boeuf, 2003).

Currently, OLEDs are the leading technology, as evidenced by their global demand and the development of many new devices based on OLED technology (Geffroy *et al.,* 2006). The advantages of OLEDs include the use of lightweight metals and organic materials, fast response times, and enhanced viewing angles (Feehery, 2007). The first OLED structure was introduced by Tang and VanSlyke (1987). Since then, industries have been actively developing this technology for displays and lighting.

The principle of OLEDs is exciton formation, in which a positive hole from the cathode combines with an electron from the anode in the organic layer (Wong and Ho, 2009). OLED devices have multilayered structures to enhance efficiency: the hole transport layer (HTL), electron transport layer (ETL), emissive layer (EML), hole injection layer (HIL), electron injection layer (EIL), electron blocking layer (EBL), and hole blocking layer (HBL); each has a special role in controlling the electrons, energy levels, and response (Khalifa *et al.*, 2004; Singh *et al.,* 2009).

Typically, OLEDs are constructed from tri (8-hydroxyquinoline) aluminum (III) (Alq_3), which is used as an emissive layer for green color and as an ETL (Montes *et al.,* 2006). Such compounds, including perylene, rubrene, and quinacridone derivatives, exhibit emission over the wavelength range of 400–600 nm (Sato *et al.,* 1998). Triphenylamine derivatives have been used as HTLs (Bellmann *et al.,* 1998). Alq3 has been used not only as the emitting layer, but also as the ETL (Cheng *et al.,* 2000). The first polymer OLED used poly(p-phenylene vinylene) (Burroughes *et al.,* 1990). Poly(p-phenylene vinylene) and polyfluorene derivatives are also widely used for OLEDs; side-chain substitutions alter the color of the emitted light (Heeger *et al.,* 1993). However, OLED materials are prone to black spot formation when exposed to oxygen or moisture, which reduces the lifetime of the device. Similar to other fabrication processes, environmental pollution, high costs, and the use of nonrenewable materials are also concerns associated with OLED fabrication. As a result, OLED studies involving naturally occurring materials, such as cytochrome c, myoglobin, hemin, chlorophyll a, and DNA, have recently been highlighted (Tajima *et al.,* 2006).DNA combined with cetyltrime thylammonium is insoluble in water, allowing its use in OLED devices (Singh *et al.,* 2009). The nucleic acid base of DNA consists of adenine, guanine, cytosine, and thymine. These constituents are used in OLEDs as the EBL, HBL, and HTL to enhance device performance; however, further optimization is required to benefit from their unique properties (Park and Lee, 2011).

In this study, an OLED device was fabricated with adenine as the electron blocking layer EBL in the OLED multilayer structure, ITO/adenine/NPB/Alq3/Al. The adenine layer thickness was varied: 1, 2, 4, and 5 nm. Thermal vacuum evaporation of adenine was carried out at two deposition rates: 0.5 and 1.0 $Å s^{-1}$. The ITO/adenine/NPB/Alq3/Al OLED samples were investigated to determine their current–voltage (*I–V*) and luminance–voltage (*L–V*) characteristics.

Materials and Methods

To fabricate the OLED devices, transparent and conductive indium tin oxide (ITO), purchased from Samsung Corning, was spin-coated onto glass substrates. The ITO layer had a surface resistance of 70±1.8 Ω and a thickness of 1850±200 Å. Photolithography was used to form a striped pattern. First, the ITO layer was coated with a photoresist (PR) developer via spin-coating, and then baked at 100°C to remove any residual solvent and to harden the surface of the PR.

Positive and negative PR processes were carried out to form the striped pattern. The positive PR was removed using ultraviolet (UV) light exposure. The patterned layer was hardened for 10 min at 130°C. The ITO layer was then etched for 3 min at 40°C, and placed into an asher for 10 min at 60°C in a nitrogen atmosphere. The patterned ITO layer was cleaned using ultrasonication for 30 min in acetone, and then in MeOH, and isopropyl alcohol for 5 min at 60°C. Finally, the specimen was exposed to the UV irradiation (184.9 nm) for 20 min at a distance of 1 cm. In a heated chamber, vacuum deposition of adenine was carried out at 5.5×10^{-6}Torr. A quartz crystal microbalance (QCM, (SQM-160, INFICON Korea)) was used to measure the thickness of the coating during vacuum deposition. The rate of the deposition rate ranged from 0.5 and 1.0 Å s^{-1}. Anadenine-based multilayer OLED structure was formed, ITO/adenine/NPB/Alq3/Al, as shown in Figure 1.The layer thicknesses of N,N′-bis (naphthalen-1-yl)-N,N′-bis(phenyl) benzidine (NPB) and Alq3 remained fixed at 40 and 60 nm, respectively. Uniform film thickness was measured using a surface profiler tool (ET-300D, Dongil Techno Co. Ltd, Korea).

The OLED devices were controlled with Lab view software (version 8.0), via a desktop personal computer equipped with a general-purposei nterfacebus (GPIB). The devices were placed in a darkroom, and current was applied using a source–measure unit (SMU) (Keithley 236). The emitted light was collected using a photodiode. The signal was converted into luminance using a picoammeter (Keithley 487).

In the experiments, the current–voltage (*I–V*) and luminance–voltage (*L–V*) characteristics of the ITO/adenine/ NPB/Alq3/Al OLED samples were measured as a function of the adenine layer thickness and adenine layer deposition rate. The adenine layer thicknesses were 1, 2, 4, and 5 nm. Thermal vacuum evaporation of adenine was carried out for two deposition rates: 0.5 and 1.0 Å s^{-1}.

Results and Discussion

Figure 2 shows the current density–voltage (*J–V*) characteristics of the ITO/ adenine/ NPB/Alq3/AlOLED as a function of adenine layer thickness (1, 2, 4 and 5 nm). The 1-nm-thick adenine layer OLED displayed a current of 1.02 mA and an operating voltage of 12.7 V. The sample with a 2-nm-thick adenine layer showed a current and operating voltage of 12.6 mA and 20 V, respectively. The ITO/adenine/NPB/Alq3/Al samples with 4- and 5-nm-thick adenine layers exhibited similar *J–V* characteristics, with the 4 nm sample having slightly higher values; a current of 18.19and 22.6 mA flowed when the operating voltage was 12and 19.1 V, respectively.

The highest luminance, 24.053 cd m^{-2} at a voltage of 15 V, was achieved for the device with a 4-nm-thick adenine layer, as shown in Figure 3. The device with a 5-nm-thickadenine layer displayed 22.195 cd m^{-2} at the same voltage (15 V). The samples with 1- and 2-nm-thick adenine layers showed luminescence only for a short time.

The Current (I)–voltage (V)I–Vand luminance–voltage (L–V) curves were measured for two deposition rates:0.5 and 1.0 Å s^{-1}**,** as shown in Figure 4. For a deposition rate of 0.5 and 1.0 Å s^{-1}, the current increased at a voltage of 1.9 and 0.5 V, respectively. At 10 V, the maximum current was 0.29 and 2.68 mA for a deposition rate of 0.5 and 1.0 Å s^{-1}**,** respectively (Figure 4).

Luminance (L)–voltage (V) curves are shown in Figure 4for the two deposition rates 0.5 and 1.0 Å s^{-1}**.** Luminance was initiated immediately for the 1.0 Å $s^{-}1$ sample and at 2.1 V for the 0.5 Å s^{-1} sample**.** At 10 V, the maximum voltage, the 0.5 and 1.0Å s^{-1} samples displayed luminance values of $3.1\times 10^{-3}$and 32.6×10^{-3} cdm^{-2}, respectively (Figure 4).

The time dependence of the electroluminescence (EL) intensity is shown in Figure 5. For the 0.5 and 1.0 Å s^{-1} samples, the minimum voltage of 10V corresponded to EL intensities of 2.04 and 2.83 arbitrary units (a.u.), respectively; the maximum voltage of 17V revealed EL intensity values of 4.72 and 4.8 a.u, respectively.

DNA and RNA, which provide the genetic blueprint for the development and function of an organism, can be obtained from a variety of sources (e.g., vegetables, fish, salmon sperm, plants, and animals) (Gomez *et al.*, 2014b). The DNA double-helix structure contains four nucleotides: adenine, guanine, cytosine, and thymine; RNA contains adenine, guanine, cytosine, and uracil. The use of biomolecules from natural substances provides an ecofriendly, low-cost means to improve the performance of OLEDs (Gomez *et al.*, 2014a, b). Many researchers have investigated DNA and RNA as alternative materials, in an attempt to find renewable constituents.

Gomez *et al.* (2011) reported that DNA became insoluble in water when combined with cetyltrimethyl ammonium; this facilitated the use of the resulting compound (CTMA complex) in OLED devices. The addition of nucleic acid bases has been shown to improve OLED performance. Adenine and thymine create EBLs and HBLs in OLEDs to control electron and whole flow, respectively; this expands the energy level between the HOMO and LUMO, resulting in high emission efficiency and luminance levels (Gomez *et al.*, 2014a, b). In those studies, the energy gap between the highest occupied molecular orbital (HOMO) and lowest unoccupied molecular orbital (LUMO) was 4.0–4.7 eV.

For commercial application, additional studies are required to optimize the manufacturing and physical parameters of OLEDs and improve device stability. In the present study, adenine was used as an EBL in the OLED device. Studies have shown that the EBL plays an important role in effectively controlling electron overflow, which limits device efficiency (Schubert *et al.*, 2007).

To find the optimum adenine thickness for the OLED device, four adenine layer thicknesses were studied: 1, 2, 4, and 5 nm. The current density (*J*)–voltage (*V*) characterization for an applied voltage of 12 V revealed the highest current density for the sample with the thinnest (1-nm-thick) adenine layer, from highest to lowest current density: 1nm> 4nm> 5nm >2nm.

Figure.1 Organic light-emitting diode (OLED) device structures of indium tin oxide/adenine/NPB/tri(8-hydroxyquinoline) aluminum(III) (ITO/adenine/NPB/Alq3/Al)

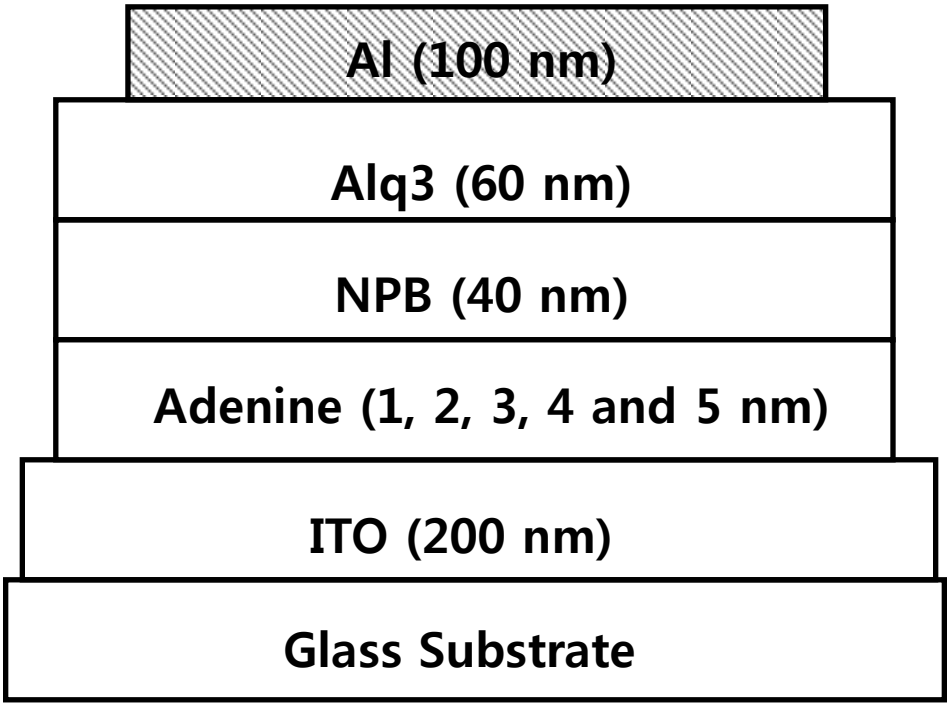

Figure.2 Current density (*J*)–voltage (*V*) (*J*–*V* curve) for ITO/adenine/NPB/Alq3/Al devices with adenine layers of various thicknesses (1, 2, 4, and 5 nm)

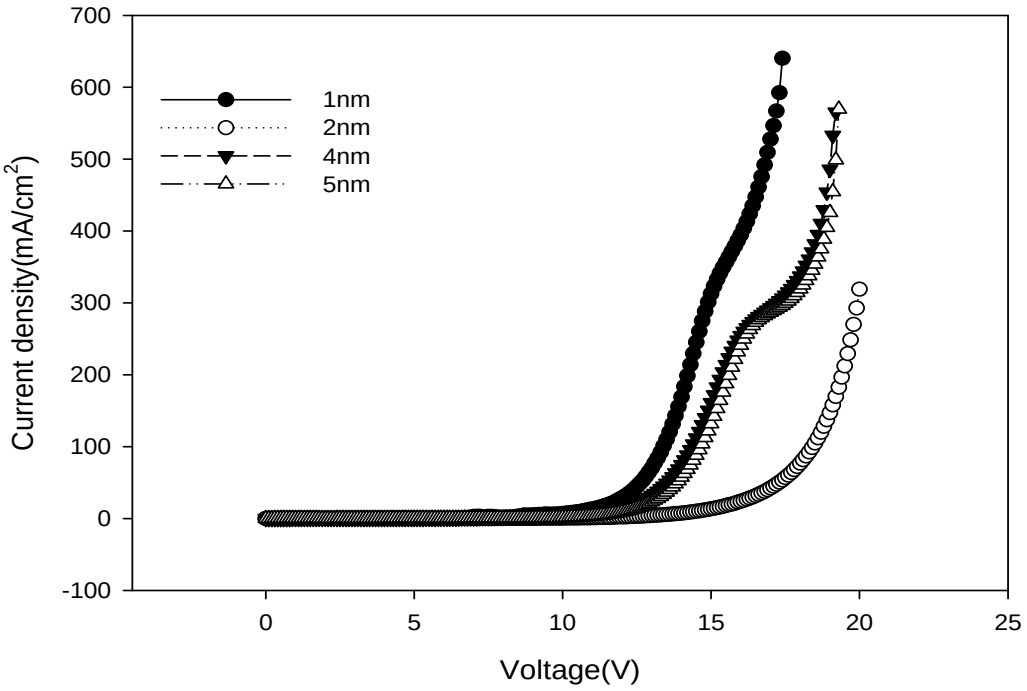

Figure.3 Luminance (*L*)–voltage (V) (*L–V* curve) for ITO/adenine/ NPB/Alq3/Al devices with adenine layers of various thicknesses (1, 2, 4, and 5 nm)

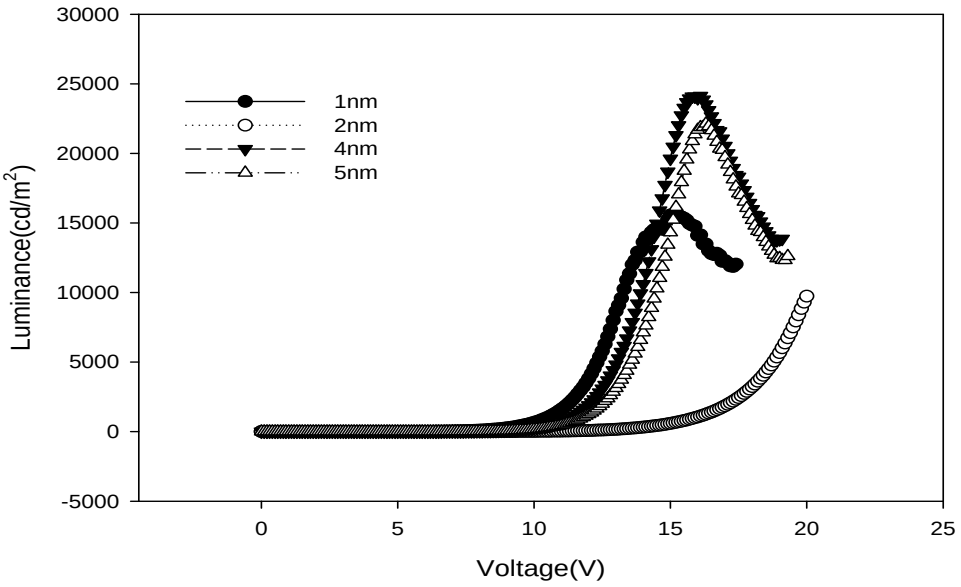

Figure.4 Current (*I*)–voltage (*V*) (*I–V*) and *L–V* curves of the OLED samples for different adenine deposition rates (0.5 and 1.0 Å s^{-1})

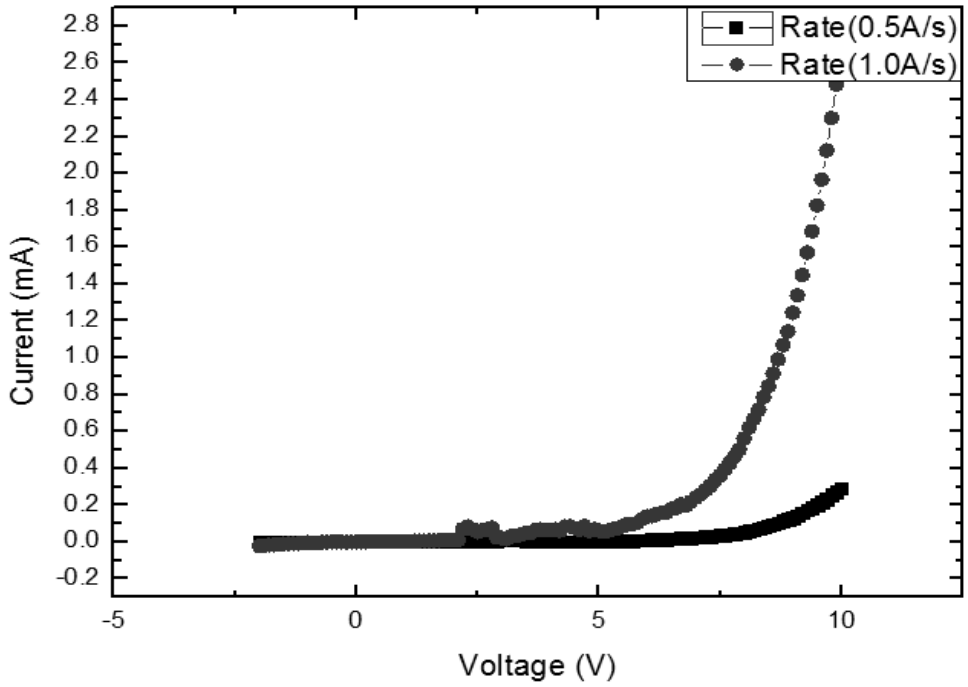

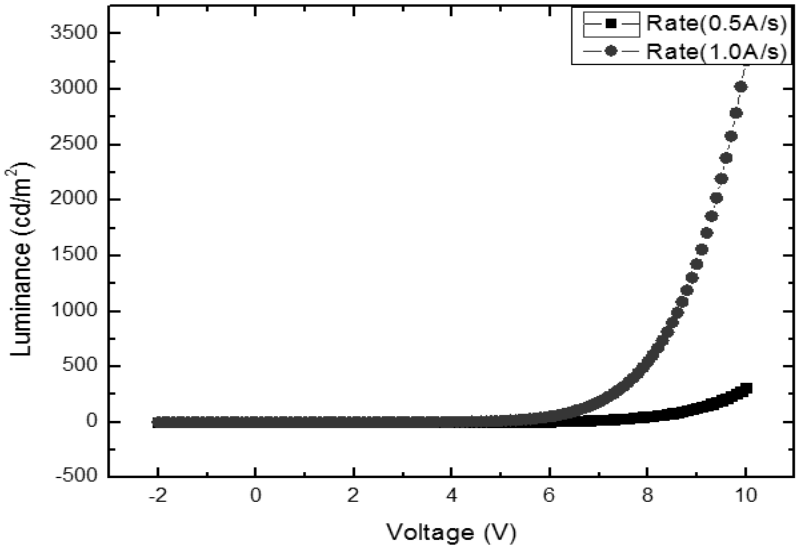

Figure.5 Electroluminance (*EL*) intensity versus time (*t*) characteristics of the OLED samples for different adenine deposition rates (0.5 and 1.0 Å s^{-1})

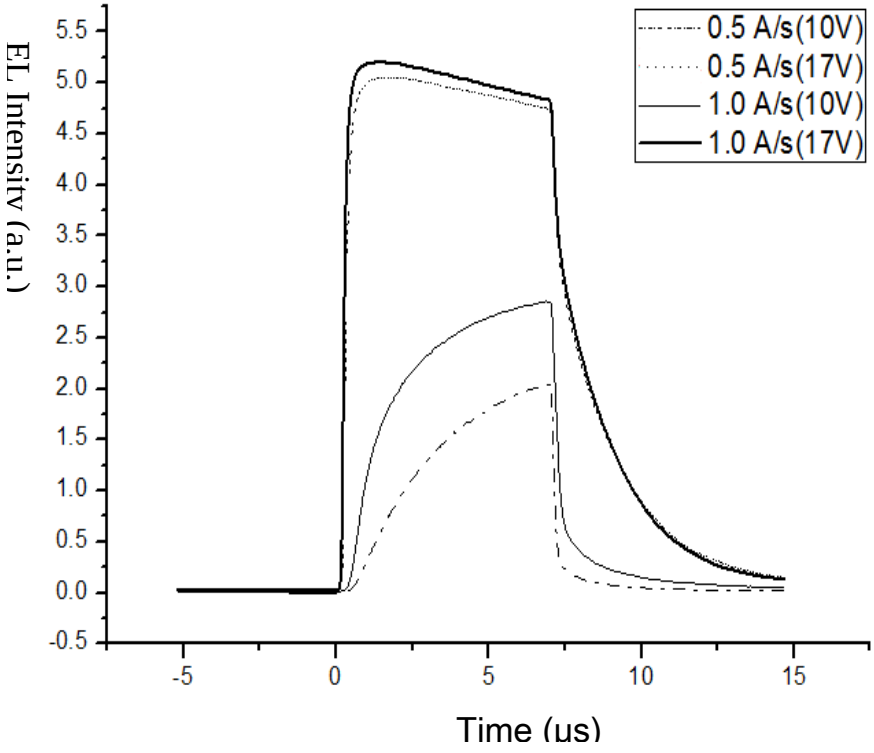

However, the highest luminance (*L*) of 24,053cdm^{-2} corresponded to an adenine layer thickness of 4nm. Gomez *et al.* (2014a, b) used an adenine layer thickness of 10 nm as an EBL in an OLED device; a luminance of 10,000cdm^{-2} was reported. Also, DNA-CTMA was 23cd/m^2 (Gomez *et al.*, 2011).

Deposition rates were affected to different quality of luminance, the rates were differentiated 0.5Å/s and 1.0Å/s. The current and luminance values given on the Results are 10 times higher for the 1.0 Å s^{-1}sample.

On the structure of Alq3 sandwiched ITO and Al, Alq3 deposition rate also conducted experiment for luminance efficiency, the rate of 1.1Å/s was shown higher luminance, the order of 1.1>1.5>0.3 Å/s (Lee *et al.*, 2004).

Cheng *et al.* (2000) also conducted same experiment, the rate from 0.05 to 1.3Å/s was better for Alq3, but the rates above 2.0Å/s decreased the luminance and photoluminescence. Generally, deposition rate are affected to the performance of OLED devices (Mandai *et al.*, 1997).

In this study, we fabricated and characterized an ITO/adenine/NPB/Alq3/Al OLED multilayered structure. The current–voltage (*I–V*) and luminance–voltage (*L–V*) characteristics were evaluated with respect to the thickness (1, 2, 4, and 5 nm) and deposition rate (0.5 and 1.0 Å s^{-1}) of the adenine layer.

The optimum adenine layer thickness and deposition rate (4 nm and 1.0 Å s^{-1}, respectively) were identified for the samples. Additional studies are required to optimize the fabrication parameters and processing steps; however, these preliminary results indicate the potential of ITO/adenine/NPB/Alq3/Al OLEDs for future OLED applications.

Acknowledgement

This research was supported by the Basic Core Technology Development Program for the Ocean and the Polar Regions of the National Research Foundation (NRF) funded by the Ministry of Science, ICT & Future Planning (2010-0020711)

References

Barbosa, V.C., Campos, L.D. 2004. A novel evolutionary formulation of the maximum independent set problem. *J. Comb. Optim.*, 8(4): 419–437.

Bellmann, E., Shaheen, S.E., Thayumanavan, S., Barlow, S., Grubbs, R.H., Marder, S.R., Kippelen, B., Peyghambarian, N. 1998. New triarylamine-containing polymers as hole transport materials in organic light-emitting diodes: effect of polymer structure and cross-linking on device characteristics. *Chem. Mater.*, 10(6): 1668–1676.

Boeuf, J.P. 2003. Plasma display panels: physics, recent developments and key issues. *J. Phys. D: Appl. Phys.*, 36(6): 53

Burroughes, J.H., Bradley, D.D.C., Brown, A.R., Marks, R.N., MacKay, K., Friend, R.H., Burns, P.L., Holmes, A.B. 1990. Light-emitting diodes based on conjugated polymers. *Nature*, 347 (6293): 539–541.

Chen, M., Zhang, F.S., Zhu, J. 2009. Lead recovery and the feasibility of foam glass production from funnel glass of dismantled cathode ray tube through pyrovacuum process. *J. Hazard. Mater.*, 161(2): 1109–1113.

Cheng, L.F., Liao, L.S., Lai, W.Y., Sun, X.H., Wong, N.B., Lee, C.S., Lee, S.T. 2000. Effect of deposition rate on the morphology, chemistry and electroluminescence of tris-(8-

hydroxyqiunoline) aluminum films. *Chem. Phys. Lett.*, 319(3): 418–422.

Feehery, W.F. 2007. Invited paper: solution processing of small-molecule OLEDs. SID symposium digest of technical papers. Blackwell publishing. 38(1): 1834–1836.

Geffroy, B., Le Roy, P., Prat, C. 2006. Organic light-emitting diode (OLED) technology: materials, devices and display technologies. *Polym. Int.*, 55(6): 572–582.

Gomez, E.F., Spaeth, H.D., Steckl, A.J., Grote, G.G. 2011. Fabrication of natural DNA-containing organic light emitting diodes. SPIE Nanoscience+ engineering. SPIE. 81030A-81030A-6

Gomez, E.F**.,** Venkatraman, V., Grote, J.G., Steckl, A.J. 2014a**.** DNA Bases thymine and adenine in bio-organic light emitting diodes. *Sci. Rep.*, 4: 1–5.

Gomez, E.F**.,** Venkatraman, V., Grote, J.G., Steckl, A.J. 2014b. Exploring the potential of nucleic acid bases in organic light emitting diodes. *Adv. Mater.*, Pp. 1–4.

Heeger, A.J. 1993. In: Salaneck, W.R., Lundstrom, I., Ranby, B. (Eds). Conjugated polymers and related materials. Oxford University Press, Oxford, Pp. 27–62.

Khalifa, M.B., Vaufrey, D., Tardy, J. 2004. Opposing influence of hole blocking layer and a doped transport layer on the performance of heterostructure OLEDs. *Org. Electron.*, 5(4): 187–198.

Lee, C.B., Uddin, A., Hu, X., Anderssonb, TG. 2004. Study of alq 3 thermal evaporation rate effects on the OLED. *Mater. Sci. Eng.*, 112(1): 14–18.

Lieberman, D. 2004. Emissive displays: a mixed bag. *J. Soc. Inf. Disp.*, 20(9): 9–18

Montes, V.A., Pohl, R., Shinar, J., Anzenbacher, P. 2006. Effective manipulation of the electronic effects and its influence on the emission of 5-substituted tris(8-quinolinolate) aluminum(III) complexes. *Cem. Eur. J.*, 12(17): 4523–4535.

Park, M.S., Lee, J.Y. 2011.Indoloacridine-based hole-transport materials for phosphorescent OLEDs with over 20% external quantum efficiency in deep blue and green. *Chem. Mater.*, 23(19): 4388–4343.

Sato, Y., Ichinosawa, S., Kanai, H. 1998. Operation characteristics and degradation of organic electroluminescent devices. *IEEE J. Sel. Top. Quantum Electron.*, 4(1): 40–48.

Singh, T.B., Sariciftciand, N.C., Grote, J.G. 2010. Bio-organic optoelectronic devices using DNA. *Org. Electron.*, 223: 73–112.

Tajima, H., Shimatani, K., Komino, T., Matsuda, M., Ikeda, S., Ando, Y., Akiyama, H. 2006. A voltage induced transition of hemin in BIODE (biomolecular light-emitting diode). *Bull. Chem. Soc. Jpn.*, 79(4): 549–554.

Tang, C.W., VanSlyke, S.A. 1987.Organic electroluminescent diodes. *Appl. Phys. Lett.*, 51(12): 913–915.

Wong, W.Y., Ho, C.L. 2009. Functional metallophosphors for effective charge carrier injection/transport: new robust OLED materials with emerging applications. *J. Mater. Chem.*, 19(26): 4457–4458.